Identification of conserved lipid/detergent-binding sites in a high-resolution structure of the membrane protein cytochrome *c* oxidase

Ling Qin[†], Carrie Hiser[†], Anne Mulichak[‡], R. Michael Garavito[†], and Shelagh Ferguson-Miller[†§]

[†]Department of Biochemistry and Molecular Biology, Michigan State University, East Lansing, MI 48824; and [‡]Industrial Macromolecular Crystallography Association–Collaborative Access Team, Advanced Photon Source, Argonne National Laboratory, Argonne, IL 60439

Edited by Harry B. Gray, California Institute of Technology, Pasadena, CA, and approved September 7, 2006 (received for review July 20, 2006)

Well ordered reproducible crystals of cytochrome *c* oxidase (C*c*O) from *Rhodobacter sphaeroides* yield a previously unreported structure at 2.0 Å resolution that contains the two catalytic subunits and a number of alkyl chains of lipids and detergents. Comparison with crystal structures of other bacterial and mammalian C*c*Os reveals that the positions occupied by native membrane lipids and detergent substitutes are highly conserved, along with amino acid residues in their vicinity, suggesting a more prevalent and specific role of lipid in membrane protein structure than often envisioned. Well defined detergent head groups (maltose) are found associated with aromatic residues in a manner similar to phospholipid head groups, likely contributing to the success of alkyl glycoside detergents in supporting membrane protein activity and crystallizability. Other significant features of this structure include the following: finding of a previously unreported crystal contact mediated by cadmium and an engineered histidine tag; documentation of the unique His–Tyr covalent linkage close to the active site; remarkable conservation of a chain of waters in one proton pathway (D-path); and discovery of an inhibitory cadmium-binding site at the entrance to another proton path (K-path). These observations provide important insight into C*c*O structure and mechanism, as well as the significance of bound lipid in membrane proteins.

cadmium binding | membrane protein structure | proton-conducting water chains

Cytochrome *c* oxidase (C*c*O) is the terminal enzyme in the electron transfer chain in eukaryotes and many bacteria. It provides the final electron sink by accepting electrons from cytochrome *c* and reducing oxygen to water (1). The energy generated from this reaction is used to translocate protons across the membrane against the membrane potential and pH gradient (2). The proton gradient so formed is then used to make ATP, a universal energy source. C*c*O is an intrinsic membrane protein with varying numbers of subunits from 3 in some bacteria to 13 in mammalian mitochondria. However, only subunits I and II, which contain the redox active heme and metal centers and are highly conserved among different species, are required for electron transfer and proton pumping activities. Other subunits, particularly the highly conserved subunit III, likely play key roles in stabilizing and regulating the enzyme activity and energy metabolism in general.

Over the past decade, several x-ray crystal structures of aa_3-type C*c*Os from bovine heart mitochondria and bacteria have been determined (3–8). However, the mechanism of vectorial translocation of protons by C*c*O remains to be solved (9). It is now recognized that water molecules play a critical role in facilitating and controlling proton transfer (10). Thus, high-resolution crystal structures of different redox states and key mutants with defined waters are necessary to elucidate the energy conservation process. However, achieving a reproducible high-resolution structure of membrane proteins remains a major challenge.

As a result of our efforts to accomplish this goal, we report a crystal structure of the two-subunit catalytic core of *Rhodobacter sphaeroides* C*c*O (I-II *Rs*C*c*O) at 2.0 Å resolution, produced from an engineered form of the enzyme and in the presence of cadmium. Unlike the crystals of the four-subunit *Rs*C*c*O (8), the two-subunit crystal form can be grown reproducibly and diffracts x-rays isotropically. A number of alkyl chains of lipids and detergents are resolved in the structure, as seen in the high-resolution bovine C*c*O (7) and in other well resolved membrane protein structures (11). But, remarkably, when the I-II *Rs*C*c*O structure is overlaid with previous structures of C*c*O from both closely [*Paracoccus denitrificans* (*Pd*)] and distantly (bovine) related species, almost all of the alkyl chain positions are found to be highly conserved, revealing specific lipid-binding sites. This finding provides perspective on the importance of lipid in membrane protein structure, function, and crystallization.

Results and Discussion

Engineering of a Molecularly Homogeneous C*c*O. Efforts to successfully crystallize *Rs*C*c*O are complicated by the inherent heterogeneity of the lipid membrane as well as the molecular heterogeneity of the protein itself. The latter is caused by the fact that (*i*) the enzyme undergoes incomplete processing of the C-terminal region of subunit II and (*ii*) there are alternative forms of subunit IV because of two translation start codons in the native gene (12). The native oxidase forms with differently processed subunits are not readily separated during purification and coexist in the crystals of the four-subunit *Rs*C*c*O, negatively affecting the quality of x-ray diffraction. To maximize the homogeneity of the protein preparation, we took two approaches. First, a 6-histidine tag was attached to the C terminus of an artificially truncated subunit II (13) (Fig. 1), providing a uniform subunit II peptide. Second, the native gene for subunit IV was deleted from the bacterial genome. In the overexpression plasmid, either no subunit IV or a shortened version was introduced, eliminating the mixture of long and short forms of subunit IV that is present in the wild-type protein. These modifications proved to be important because the I-II subunit crystals did not form when there were significant amounts of the longer subunit IV in the enzyme complex.

Author contributions: L.Q., R.M.G., and S.F.-M. designed research; L.Q., C.H., and A.M. performed research; C.H. contributed new reagents/analytic tools; L.Q., A.M., and R.M.G. analyzed data; and L.Q., C.H., R.M.G., and S.F.-M. wrote the paper.

The authors declare no conflict of interest.

This article is a PNAS direct submission.

Freely available online through the PNAS open access option.

Abbreviations: *Rs*, *R. sphaeroides*; *Pd*, *P. denitrificans*; CcO, cytochrome *c* oxidase; I-II *Rs*CcO, the two-subunit version of *Rs*CcO; LDAO, lauryldimethylamine-oxide.

Data deposition footnote: The complete coordinates and structure factors have been deposited in the Protein Data Bank, www.pdb.org (PDB ID code 2GSM).

[§]To whom correspondence should be addressed. E-mail: fergus20@msu.edu.

BIOCHEMISTRY

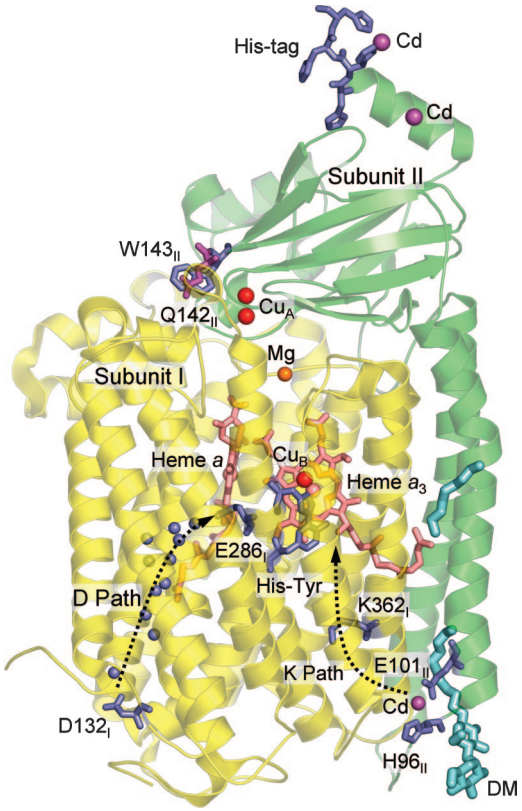

Fig. 1. Important structural features of the two-subunit *Rs*CcO. Subunit I is shown in yellow, and subunit II is shown in green. Residues of interest are shown in stick models and colored blue, except for $Q142_{II}$, which is colored magenta for clarity. Heme groups are shown in salmon. Metals are shown as spheres and colored as follows: Fe, salmon; Cu, red; Mg, blue; Cd, magenta. Two proton uptake pathways are indicated by dotted arrows, with resolved waters in the D path shown as blue spheres. One of the resolved detergent molecules (DM-decyl maltoside), corresponding to the DM at the phosphatidyl choline (PC) site in Fig. 3*C*, is shown in cyan, as is one of the alkyl chains corresponding to the cardiolipin (CDL) site in Fig. 3*B*.

Minimizing Loss of Lipid During Purification. A purification procedure was designed to reduce detergent exposure and the number of steps of chromatography to retain native lipid. [Adding back lipids (14) was not found to improve resolution in this case.] Controlling the exact protein/detergent ratio during purification was critical in crystal formation. A previous standard purification of *Rs*C*c*O involved two nickel affinity columns and one ion exchange (8). Our revised protocol involves only one column chromatography by nickel affinity with a modified two-step gradient (see *Supporting Methods*, which is published as supporting information on the PNAS web site). The purity was not quite as high as in the routine purification, but the visible spectral characteristics were the same (Fig. 8 *Top*, which is published as supporting information on the PNAS web site).

Formation of a Two-Subunit Crystal with Isotropic Diffraction and a Cadmium/His-Tag Crystal Contact. In a previous study (6), the I-II subunit crystal of C*c*O from *P. denitrificans* (*Pd*C*c*O) was purposely obtained by using the strong detergent lauryldimethylamine-oxide (LDAO) to remove subunits III and IV (6). In the case of *Rs*C*c*O, crystals of the I-II subunit complex emerged spontaneously and reproducibly, from the purified, engineered enzyme with either three or four subunits, in the presence of cadmium ion (see *Methods* and *Supporting Methods*). Fig. 1 shows the overall structure of the form.

Loss of subunit III/IV during the crystallization procedure

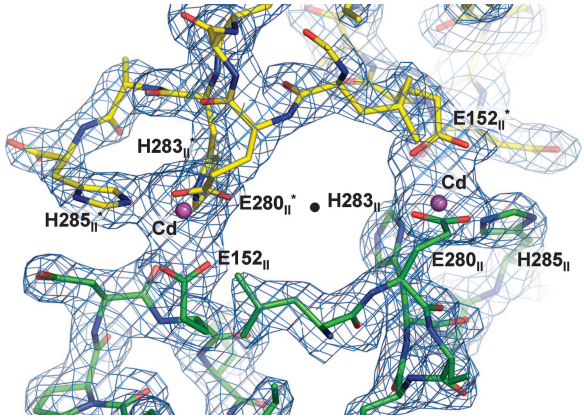

Fig. 2. Major crystal contact region of I-II *Rs*C*c*O contributed by two engineered histidine tags at the C terminus of subunit II and two cadmium ions. One *Rs*C*c*O molecule is colored by atom type (C, green; O, red; N, blue); the other molecule is colored similarly but C is yellow. Cadmium is purple. The $(2F_o - F_c)$ electron density map contoured at 1.3σ is shown in blue. The participating amino acid residues from the two protein molecules form a tetrahedral coordination around the cadmium ion as labeled in the figure. There are two identical crystal contact interactions at this interface with a quasi-2-fold rotational symmetry axis (shown as a black dot) at the center perpendicular to the plane of the paper.

may arise from the presence of cadmium, added in an effort to locate the site of inhibition of C*c*O by Zn^{2+} and Cd^{2+}. In the four-subunit crystal form of *Rs*CcO, we have found two cadmium-binding sites in subunit III (unpublished data), which may increase its already strong propensity to dissociate (15, 16). The short version of subunit IV is also likely to be more labile because of reduced protein:protein contact.

Compared with the four-subunit *Rs*CcO crystals, which quickly dissolved upon raising the temperature above 4°C, the I-II *Rs*C*c*O crystals are stable and can be reproducibly grown at room temperature, although those grown at 4°C diffract better. Furthermore, the crystals of four-subunit *Rs*C*c*O displayed considerable anisotropic x-ray diffraction, which resulted in limiting the resolution to 2.3 Å along a^* and b^*, but only to 2.8 Å along c^* (8). In contrast, the crystals of the I-II subunit form display no significant diffraction anisotropy to 2.0 Å resolution. An analysis of the crystal contacts reveals a major contact region involving the extramembrane domain of subunit II that is mediated by two cadmium ions and two histidine tags (Fig. 2). Each cadmium ion is liganded in a tetrahedral coordination geometry by three amino acid side chains from one *Rs*C*c*O molecule, including a glutamate and two histidines from the histidine tag and a glutamate residue from another *Rs*C*c*O molecule. An identical contact exists close by, involving the histidine tag and the same residues from the neighboring *Rs*C*c*O molecule in the asymmetric unit. This strong contact may be responsible for the superior x-ray diffraction properties and stability of the I-II subunit crystals.

Structural and Biochemical Characteristics of the I-II *Rs*C*c*O Crystals. As in the case of the two-subunit *Pd*C*c*O obtained under very different conditions (6), the I-II *Rs*C*c*O is structurally similar to the core of the four-subunit enzyme. The redox active metal centers found in the four-subunit structures are all present in the I-II subunit structure (Fig. 1), with identical ligations. Unlike the four-subunit crystal structure, there are two independent I-II *Rs*C*c*O molecules in the asymmetric unit, and the structures are slightly different in terms of resolution of water and other bound molecules.

The redissolved I-II *Rs*C*c*O crystals are highly active and display native spectral characteristics (Fig. 8). The enzymatic

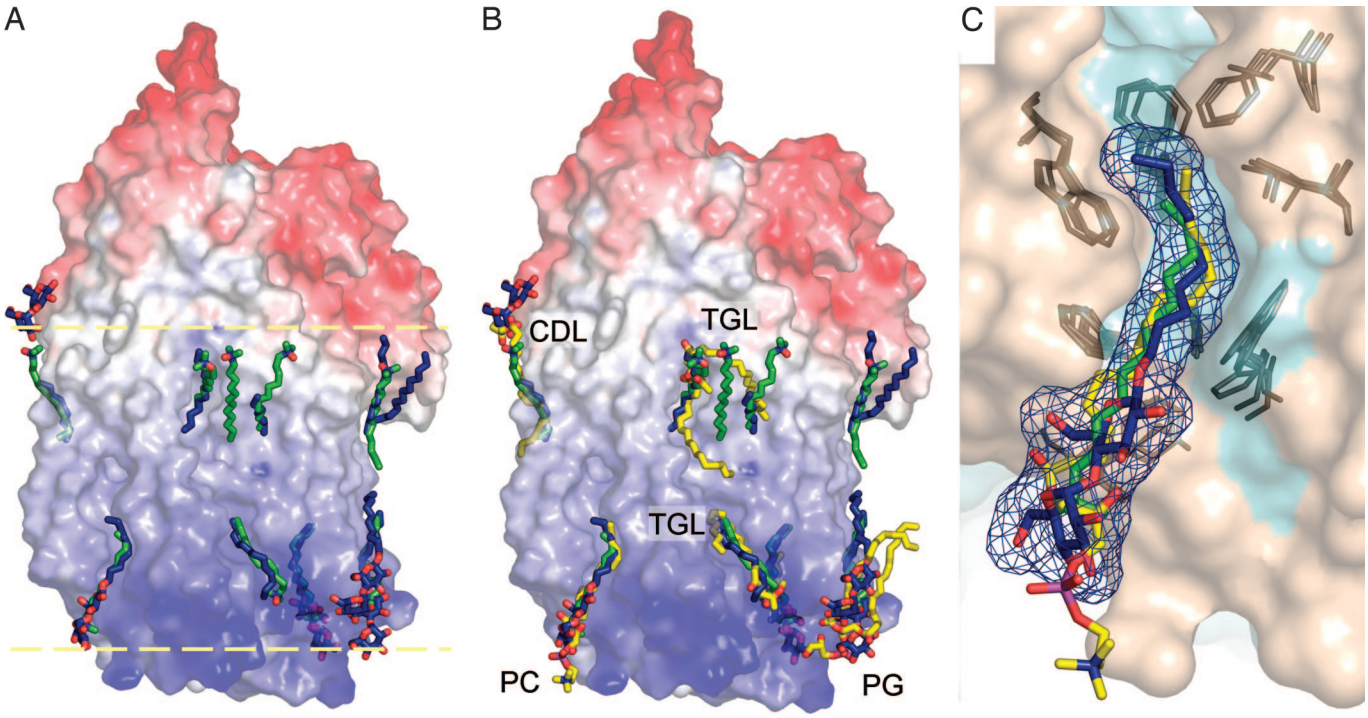

Fig. 3. Surface representations of I-II *Rs*CcO illustrating the position and superposition of detergent/lipid molecules in *Rs*, *Pd*, and bovine CcO structures. The superpositions were identified by overlaying the structures of I-II *Rs*CcO, I-II *Pd*CcO (PDB ID code 1AR1), and bovine heart mitochondrial CcO (PDB ID code 1V54). (*A*) Molecular surface representations of I-II *Rs*CcO, colored by relative electrostatic potential (blue, positive; red, negative) and showing the detergent molecules, maltose headgroups, and alkyl chains resolved in the structure (C, dark blue; O, red), superimposed on the LDAO detergent molecules resolved in the I-II *Pd*CcO structure (C, green; O, red; N, blue). The lipid bilayer region is represented by two yellow dashed lines. (*B*) Lipid molecules in the bovine CcO structure that occupy the same sites as alkyl chains resolved in *Rs*/*Pd* structures are shown (C, yellow). Structures of *Rs*CcO and *Pd*CcO are colored as in *A*. PC, phosphatidyl choline; PG, phosphatidyl glycerol; CDL, cardiolipin; TGL, triacylglycerol. (*C*) Detailed view of one of the conserved lipid-binding sites, where an alkyl chain of phosphatidyl choline resolved in bovine CcO occupies the same site as detergents resolved in *Rs*CcO and *Pd*CcO. Surface representation of I-II *Rs*CcO is colored by subunits (subunit I, cyan; subunit II, wheat). The decyl maltoside from *Rs*CcO, the detergent LDAO from *Pd*CcO, and the partial lipid molecule in bovine CcO are colored by atom type as above. The mesh representation of the resolved decyl maltoside is shown in blue. Some well conserved residues in all three structures surrounding the alkyl chain-binding site are colored dark gray.

activity decreases as the enzyme turns over in steady-state measurements, a phenomenon typical of C*c*O missing subunit III (17) (Fig. 9, which is published as supporting information on the PNAS web site). Adding lipid and arachidonic acid protects the enzyme from undergoing this "suicide" inactivation (18) (Fig. 9). The initial activity is similar to that reported for purified subunit III-minus enzyme, even though these crystals had been maintained under crystallization conditions for ≈3 months before being dissolved and assayed. The high activity observed supports previous conclusions that the subunit III-minus oxidase is very stable unless it is undergoing turnover (18).

Conserved Sites of Detergent and Lipid Interaction. Beyond providing a hydrophobic solvent and diffusion barrier, many studies suggest that membrane lipids can contribute to functional aspects of associated proteins (19, 20). Only recently has it been possible to obtain high enough resolution crystal structures of membrane proteins to identify bound lipids. The significance of the associated lipids is only beginning to be recognized (19, 20).

In the crystal structure of the four-subunit *Rs*C*c*O, a total of six phosphatidyl ethanolamines were identified, four surrounding subunit IV and two associated with subunits III and I (8). Subunit IV interacts with its neighboring subunits almost entirely via lipid molecules (8), emphasizing the integral nature of the lipid. In the I-II *Rs*C*c*O structure, all these lipids are lost, not surprisingly because they are most strongly associated with the missing subunits. However, in other locations, there are well resolved detergent molecules, as well as a number of tube-like electron densities interpreted as hydrocarbon tails of either native membrane lipids or detergent molecules, because they are found in the transmembrane region of the enzyme (Figs. 3*A* and 4). The headgroups of these hydrocarbon tails are not resolved, suggesting that they are flexible, possibly because of the high salt concentration in the crystallization medium. This phenomenon of unresolved head groups was observed in the case of lipids identified in bacteriorhodopsin, even at 1.55 Å resolution (11).

An interesting observation was made when the crystal structures of the I-II C*c*O enzymes from *Rs* and *Pd* (6) were overlaid (Fig. 3*A*). In both cases, alkyl chains are resolved in the region where membrane lipids would normally interact. Surprisingly, many of the chains occupy essentially identical positions on the surface of the two proteins, despite the fact that the structures are from different species and underwent different purification and crystallization procedures by using different detergents. The implication is that these locations are conserved sites for specific interactions of membrane lipids with the transmembrane protein surface.

Indeed, superposition of the I-II *Rs*CcO structure on the 1.8-Å resolution bovine heart C*c*O structure, in which 13 lipids are resolved (7), reveals that most of the alkyl chains in I-II *Rs*C*c*O coincide not only with those in the *Pd*C*c*O but also with chains of lipid molecules in bovine C*c*O, as shown in Fig. 3*B*. A closer view in Fig. 3*C* shows the crevice occupied by a decyl maltoside in *Rs*C*c*O, an LDAO detergent in *Pd*C*c*O, and one of the alkyl tails of a phosphatidyl choline in bovine C*c*O. Also illustrated are residues that seem to be involved in creating the lipid crevice,

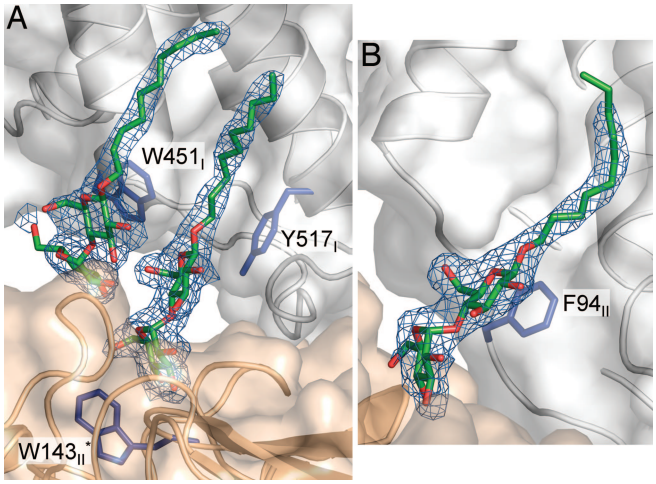

Fig. 4. Characteristics of detergent molecules resolved in the I-II *Rs*CcO structure. (*A*) Two decyl maltoside detergent molecules (colored by atom type: C, green; O, red; N, blue) resolved at the interface of two *Rs*CcO molecules (gray and wheat). The ($2F_o - F_c$) difference electron density map (dark blue) surrounding the decyl maltosides contoured at 1.3 σ is shown. Tyrosine and tryptophan residues (blue) were found stacking with the head groups of the two decyl maltosides. (*B*) One decyl maltoside resolved on another location, also at molecular interface. The ($2F_o - F_c$) difference electron density map (dark blue) contoured at 1.0σ is shown. Phenylalanine residue (blue) was found forming a stacking interaction with the sugar ring.

which are well conserved in all three C*c*O structures. Similar conservation can be found for residues in the vicinity of two other decyl maltosides occupying roughly the same sites as the alkyl tails of a phosphatidyl glycerol molecule resolved in bovine C*c*O (Fig. 10*A*, which is published as supporting information on the PNAS web site).

In other locations, resolved alkyl tails in I-II *Rs*C*c*O and *Pd*C*c*O also correspond to lipids in bovine C*c*O, such as a cardiolipin molecule in the bovine C*c*O structure (Figs. 3*B* and 10*B*). Cardiolipin has been implicated in the function of electron transfer complexes in the respiratory chain (19, 20), and our mass spectrometric analyses consistently show the preferential retention of cardiolipin in the purified *Rs*C*c*O enzyme and in redissolved crystals (X. Zhang, L.Q., and S.F.-M., unpublished data). Therefore, the alkyl tail resolved here could indeed be from the bound cardiolipin molecule at this conserved site. The highly ionic cardiolipin head group and flexible, unsaturated alkyl tails may account for incomplete resolution under the crystallization conditions.

Where decyl maltoside detergents are resolved (Fig. 4), nearby aromatic residues form stacking interactions between the sugar rings and the aromatic rings. The same intimate interaction can be observed in a number of other membrane protein structures (21, 22). Alkyl glycoside headgroups seem to mimic phosphatidyl head groups in their well known interactions with tryptophan and tyrosine (19, 23). Their ability to effectively occupy specific lipid-binding sites may account for their success in stabilizing and crystallizing membrane proteins. These observations suggest that detergent molecules resolved in a membrane protein structure likely reveal where a phospholipid should be bound. In support of this idea is the observation that surface regions in I-II *Rs*C*c*O that were originally covered by subunits III and IV show no lipid/detergent-binding sites (data not shown).

The above findings strongly support a conclusion that there are specific, conserved interaction sites for lipids on membrane proteins and that a detergent with the right properties can at least partially occupy the same site.

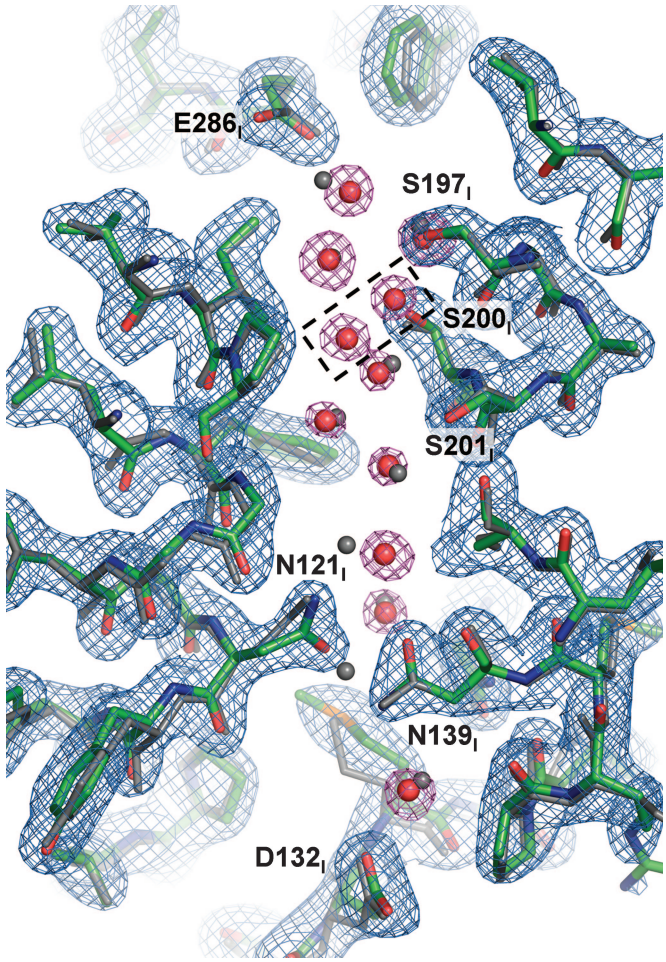

Fig. 5. Comparison of the resolved waters in the D proton uptake pathway in the crystal structures of I-II *Rs*CcO and the four-subunit *Rs*CcO. The I-II *Rs*CcO structure is colored by atom type (C, green; O, red; N, blue), and the structure of the four-subunit *Rs*CcO (PDB ID code 1M56) is colored gray. Waters in I-II *Rs*CcO structure are red; waters in four-subunit *Rs*CcO are gray. The dotted black box indicates two additional waters resolved in the I-II *Rs*CcO. The ($2F_o - F_c$) difference electron density map contoured at 1.0σ is shown in blue and magenta.

Conserved Waters in Proton Pathways. There are two established proton pathways in the enzyme: D and K pathways, named after the residues D132$_I$ and K362$_I$, whose mutational replacement blocks each path (24–26) (Fig. 1). In the four-subunit *Rs*C*c*O crystal structure (8), a clear chain of waters was resolved in the D pathway from D132$_I$ leading to the vicinity of E286$_I$, a residue thought to be critical in conducting protons to the active site and to the external bulk phase (27).

In the current structure, the chain of waters is again clearly resolved. Fig. 5 shows the comparison of the resolved D channel waters in the I-II subunit and four-subunit *Rs*C*c*O structures. The positions of the waters and the conformations of the amino acid residues along the pathway are very similar between the two structures except for N121$_I$, which is reoriented. This observation is consistent with the lack of one water in the I-II *Rs*C*c*O structure, which is liganded to the N121$_I$ side chain in the four-subunit structure. There are two additional waters resolved in the I-II subunit structure further up in the pathway close to S200$_I$ (Fig. 5, box). The high degree of conservation of these ordered, hydrogen-bonded waters is consistent with their importance in determining rate and directionality of proton movement. The slight difference between the four-subunit and I-II

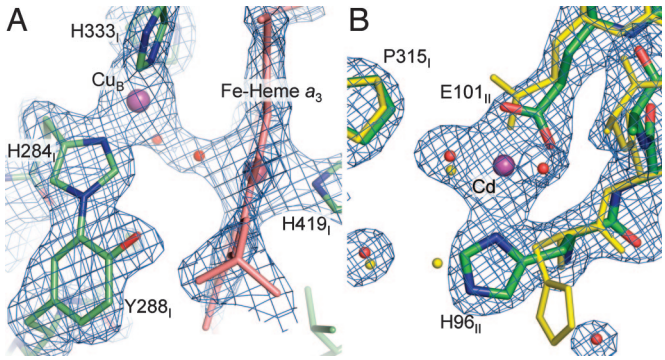

Fig. 6. Detailed structure of the metal ligands at the active site (*A*) and the inhibitory cadmium-binding site (*B*). (*A*) The covalent linkage between ring atoms of $Y288_I$ and $H284_I$. The ($F_o - F_c$) difference simulated annealing omit map is shown in blue, contoured at 4.0 σ, calculated by omitting Cu_B, $H284_I$, $Y288_I$, Fe of Heme a_3, and all residues including heme a_3 that have atoms closer than 3 Å to them. The amino acid residues are colored by atom type (C, green; O, red; N, blue), the heme group is colored light red, and the Cu_B atom is colored purple. The ligands tentatively assigned as a water bound to heme a_3-Fe and an OH^- group bound to Cu_B are both colored in red. (*B*) An inhibitory cadmium-binding site in the structure of I-II *Rs*C*c*O. The ($2F_o - F_c$) difference electron density map contoured at 1.3σ is shown. In the current structure (colored by atom type: C, green; O, red; N, blue), cadmium (purple) is bound to $E101_{II}$ and $H96_{II}$ of subunit II. Binding of cadmium alters the conformations of the ligating residues compared with that found in the unliganded four-subunit *Rs*C*c*O crystal structure (yellow).

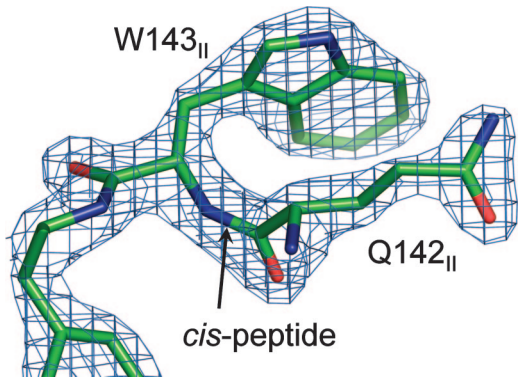

Fig. 7. The cis-peptide bond found between $Q142_{II}$ and $W143_{II}$. The structure is colored by atom type (C, green; O, red; N, blue). The ($2F_o - F_c$) difference electron density map contoured at 1.3σ is shown in blue.

subunit structure in the water arrangement in the D pathway could be related to the absence of subunit III. Although not essential for either electron transfer or proton pumping, subunit III is in close proximity to the D pathway and seems to play a role in the kinetics of proton uptake by this channel (28). The K pathway has few waters resolved in the four-subunit structure (8), but again their positions are conserved in the I-II subunit *Rs*C*c*O structure. Overall, there is remarkable conservation of water positions in the C*c*O structures, suggesting a critical role of water in proton transfer (10).

Structure of the Active Site: Bridging Ligand and His–Tyr Covalent Linkage. Heme a_3 and Cu_B form the active site of the enzyme where oxygen is reduced to water. A unique covalent linkage between the Cε_2 of $Y288_I$ and the Nε_2 of a Cu_B ligand, $H284_I$, is observed in the crystal structures of C*c*O from bovine heart and *Pd* (4, 6), and its presence is supported by mass spectrometry analysis (29). The linkage was not resolved unequivocally in the crystal structure of the four-subunit *Rs*C*c*O. A mixture of covalently linked and noncovalently linked species could account for the observed density, calling into question the functional significance of the cross-link (8). In the current structure, well resolved electron density that is best fit by the cross-linked form is observed between the Nε_2 of $H284_I$ and Cε_2 of $Y288_I$ in a simulated annealing omit map contoured at 4.0 σ (Fig. 6*A*). This finding supports the concept that the covalently linked His-Tyr is important in the catalytic mechanism; the adduct is proposed to lower the pK_a of the tyrosine OH group and facilitate free radical formation of $Y288_I$ (4, 30).

Between the Fe in the heme a_3 and the Cu_B center, there is residual density in the ($F_o - F_c$) map. Previously, observed density in this region has been interpreted as a water molecule ligated to Fea_3 and a hydroxide ion to Cu_B (6) or a peroxy-bridge in the binuclear center (4). It is difficult to unambiguously assign the position and identity of the ligands in this pocket because of the presence of heavy atoms of Fe and Cu, as well as the uncertainty regarding the redox state during x-ray analysis. Although the peroxy-bridge seems to fit the electron density fairly well, the presence of such a peroxy form is not expected in the oxidized enzyme. We tentatively interpret this electron density as a hydroxide bound to Cu_B and a less well resolved water molecule bound to heme a_3-Fe (Fig. 6*A*).

Inhibitory Cadmium-Binding Site. It was previously observed that Zn^{2+} or Cd^{2+} inhibits C*c*O activity both in the purified state and in reconstituted lipid vesicles under steady-state turnover (31). Besides the cadmium-binding sites found at the crystallographic interface, an additional cadmium-binding site was identified in both *Rs*C*c*O molecules, involving side chain atoms of $E101_{II}$ and $H96_{II}$, as shown in Figs. 1 and 6*B*. This cadmium-binding site was confirmed by anomalous difference Fourier map and was also observed in the structure of the four-subunit *Rs*C*c*O when the crystal was soaked in a $CdCl_2$ solution before flashcooling (unpublished data). $E101_{II}$ has been suggested to be the proton entry point for the K pathway in *Rs*C*c*O (32). The observed cadmium-binding site could account for the inhibition of activity of the purified enzyme, by blockage of the K pathway for proton uptake. It is likely, however, that the observed Zn^{2+}/Cd^{2+} inhibitory effect on the enzyme involves more than one site (33). The lack of binding of Zn^{2+}/Cd^{2+} at the opening of the D path in this crystal structure could be due to the loss of subunit III, which provides several histidines close to the D channel entrance.

Cis-Peptide Bond Between $Q142_{II}$ and $W143_{II}$ at the Electron Transfer Interface. Electrons enter C*c*O from cytochrome *c* at the Cu_A center, apparently via the indole ring of a tryptophan residue, $W143_{II}$ (34–36). $W143_{II}$ and $Q142_{II}$ are highly conserved and at the center of the predicted interface between cytochrome *c* and C*c*O (37). Interestingly, the peptide bond between $Q142_{II}$ and $W143_{II}$ is a cis-peptide bond (Fig. 7). This cis-peptide bond has not been previously noted in C*c*O; it is often missed because of its rare occurrence (38). The presence of such a bond is important in orienting the side chains of flanking residues in the same direction, in this case toward the proposed cytochrome *c*-binding site, and permitting close association between the indole ring and the glutamine through dipole–quadrupole interaction (38). A role in facilitating the electron conducting interface may be surmised.

Summary. Reproducible, well ordered crystals of a two-subunit *Rs*C*c*O provide important insight into its structure, function, and specific association with lipid and water. The observations of conserved water positions and conserved sites for lipid or detergent reveal a critical role for specifically bound "solvent" molecules in membrane protein structure and activity.

Methods

The detailed descriptions of molecular cloning, protein purification, crystallization, x-ray diffraction data collection, and structure determination are included in *Supporting Methods*. Dodecyl maltoside and Ni-NTA were used in purification, and decyl and dodecyl maltoside were used in crystallization. X-ray diffraction data were collected on a single frozen crystal at Beamline 5ID-B [Dupont–Northwestern–Dow (DND) Collaborative Access Team (CAT), Advanced Photon Source (APS)]. The structure was determined by molecular replacement by using the published four-subunit *Rs*C*c*O structure (PDB ID code 1M56) as the starting search model. Structural refinement was performed by using CNS and Refmac5, with final R_{work} and R_{free} factors of 21.4% and 23.2%, respectively. The anomalous diffraction data were collected at Beamline 23ID-D [General Medicine and Cancer Institutes (GM/CA)-CAT, APS]. The x-ray data collection and refinement statistics are listed in Table 1, which is published as supporting information on the PNAS web site.

We thank Drs. Kaillathe Padmanabhan, Rachel Powers, Christine Harman, and Nicole Webb for helpful discussions and suggestions regarding data collection and structural refinement; Xi Zhang, Dr. Yasmin Hilmi, Dr. Steve Seibold, and Sarah House for contributions; staff from GM/CA-CAT, DND-CAT, and Life Sciences (LS)-CAT at APS for assistance at the synchrotron facility; Dr. Zdzislaw Wawrzak from DND-CAT, APS for the initial processing of x-ray diffraction data; and Drs. Margareta Svensson-Ek, So Iwata, and Peter Brzezinski for support and collaboration. This work was funded by National Institutes of Health (NIH) Grant GM26916, Human Frontier Science Program Grant RG315/2000-M, Michigan Technology TriCorridor Center for Structural Biology, Core Technology Alliance Grant 085P1000817, NIH Grant P01GM57323, and Michigan State University Grant REF03-016.

1. Ferguson-Miller S, Babcock GT (1996) *Chem Rev (Washington, DC)* 96:2889–2907.
2. Wikstrom MK (1977) *Nature* 266:271–273.
3. Iwata S, Ostermeier C, Ludwig B, Michel H (1995) *Nature* 376:660–669.
4. Yoshikawa S, Shinzawa-itoh K, Nakashima R, Yaono R, Yamashita E, Inoue N, Yao M, Fei MJ, Libeu CP, Mizushima T, *et al*. (1998) *Science* 280:1723–1729.
5. Tsukihara T, Aoyama H, Yamashita E, Tomizaki T, Yamaguchi H, Shinzawa-Itoh K, Nakashima R, Yaono R, Yoshikawa S (1996) *Science* 272:1136–1144.
6. Ostermeier C, Harrenga A, Ermler U, Michel H (1997) *Proc Natl Acad Sci USA* 94:10547–10553.
7. Tsukihara T, Shimokata K, Katayama Y, Shimada H, Muramoto K, Aoyama H, Mochizuki M, Shinzawa-itoh K, Yamashita E, Yao M, *et al*. (2003) *Proc Natl Acad Sci USA* 100:15304–15309.
8. Svensson-Ek M, Abramson J, Larsson G, Tornroth S, Brzezinski P, Iwata S (2002) *J Mol Biol* 321:329–339.
9. Mills DA, Ferguson-Miller S (2003) *FEBS Lett* 545:47–51.
10. Sharpe MA, Qin L, Ferguson-Miller S (2005) in *Biophysical and Structural Aspects of Bioenergetics*, ed Wikstrom M (R Soc Chem, Cambridge, UK), pp 26–54.
11. Luecke H, Schobert B, Richter H-T, Cartailler J-P, Lanyi JK (1999) *J Mol Biol* 291:899–911.
12. Distler AM, Allison J, Hiser C, Qin L, Hilmi Y, Ferguson-Miller S (2004) *Eur J Mass Spectrom* 10:295–308.
13. Hiser C, Mills DA, Schall M, Ferguson-Miller S (2001) *Biochemistry* 40:1606–1615.
14. Zhang H, Kurisu G, Smith JL, Cramer WA (2003) *Proc Natl Acad Sci USA* 100:5160–5163.
15. Thompson DA, Ferguson-Miller S (1983) *Biochemistry* 22:3178–3187.
16. Bratton MR, Pressler MA, Hosler JP (1999) *Biochemistry* 38:16236–16245.
17. Hosler JP (2004) *Biochim Biophys Acta* 1655:332–339.
18. Mills DA, Hosler JP (2005) *Biochemistry* 44:4656–4666.
19. Palsdottir H, Hunte C (2004) *Biochim Biophys Acta* 1666:2–18.
20. Hunte C (2005) *Biochem Soc Trans* 33:938–942.
21. Snijder HJ, Van Eerde JH, Kingma RL, Kalk KH, Dekker N, Egmond MR, Dijkstra BW (2001) *Protein Sci* 10:1962–1969.
22. Okada T, Fujiyoshi Y, Silow M, Navarro J, Landau EM, Shichida Y (2002) *Proc Natl Acad Sci USA* 99:5982–5987.
23. Yau W-M, Wimley WC, Gawrisch K, White SH (1998) *Biochemistry* 37:14713–14718.
24. Garcia-Horsman JA, Puustinen A, Gennis RB, Wikstrom M (1995) *Biochemistry* 34:4428–4433.
25. Fetter JR, Qian J, Shapleigh J, Thomas JW, Garcia-Horsman A, Schmidt E, Hosler J, Babcock GT, Gennis RB, Ferguson-Miller S (1995) *Proc Natl Acad Sci USA* 92:1604–1608.
26. Thomas JW, Lemieux LJ, Alben JO, Gennis RB (1993) *Biochemistry* 32:11173–11180.
27. Hofacker I, Schulten K (1998) *Proteins Struct Funct Genet* 30:100–107.
28. Mills DA, Tan Z, Ferguson-Miller S, Hosler J (2003) *Biochemistry* 42:7410–7417.
29. Buse G, Soulimane T, Dewor M, Meyer HE, Bluggel M (1999) *Protein Sci* 8:985–990.
30. Proshlyakov DA, Pressler MA, DeMaso C, Leykam JF, DeWitt DL, Babcock GT (2000) *Science* 290:1588–1591.
31. Mills DA, Schmidt B, Hiser C, Westley E, Ferguson-Miller S (2002) *J Biol Chem* 277:14894–14901.
32. Branden M, Tomson F, Gennis RB, Brzezinski P (2002) *Biochemistry* 41:10794–10798.
33. Aagaard A, Namslauer A, Brzezinski P (2002) *Biochim Biophys Acta* 1555:133–139.
34. Witt H, Malatesta F, Nicoletti F, Brunori M, Ludwig B (1998) *J Biol Chem* 273:5132–5136.
35. Zhen Y, Hoganson CW, Babcock GT, Ferguson-Miller S (1999) *J Biol Chem* 274:38032–38041.
36. Wang K, Zhen Y, Sadoski R, Grinnell S, Geren L, Ferguson-Miller S, Durham B, Millett F (1999) *J Biol Chem* 274:38042–38050.
37. Roberts VA, Pique ME (1999) *J Biol Chem* 274:38051–38060.
38. Jabs A, Weiss MS, Hilgenfeld R (1999) *J Mol Biol* 286:291–304.